

Lattice constant of Al-rich α -phase in equilibrium with different precipitates in Al-Zn alloys

Popović, Stanko; Gržeta, Biserka; Löffler, Hans; Wendrock, Gottfried

Source / Izvornik: **Fizika A**, 1995, 4, 529 - 538

Journal article, Published version

Rad u časopisu, Objavljena verzija rada (izdavačev PDF)

Permanent link / Trajna poveznica: <https://um.nsk.hr/um:nbn:hr:217:244551>

Rights / Prava: [In copyright](#)/[Zaštićeno autorskim pravom.](#)

Download date / Datum preuzimanja: **2025-03-02**



Repository / Repozitorij:

[Repository of the Faculty of Science - University of Zagreb](#)



LATTICE CONSTANT OF Al-RICH α -PHASE IN EQUILIBRIUM WITH
DIFFERENT PRECIPITATES IN Al-Zn ALLOYS

STANKO POPOVIĆ^(a,b), BISERKA GRŽETA^(b), HANS LÖFFLER^(c) and
GOTTFRIED WENDROCK^(c)

^(a)*Physics Department, Faculty of Science, 10001 Zagreb, P.O.B.162, Croatia*

^(b)*Ruder Bošković Institute, 10001 Zagreb, P.O.B.1016, Croatia;*

^(c)*Martin-Luther Universität, D-06099 Halle (Saale), P.F.8, Germany*

Dedicated to Professor Mladen Paić on the occasion of his 90th birthday

Received 15 June 1995

UDC 548.73

PACS 61.50.-f, 64.70, 64.75.-p, 64.75.+g, 65.70.+y

A series of Al-rich Al-Zn alloys were studied by X-ray diffraction at room and elevated temperatures. Using the present results and those cited in literature, the following conclusion can be drawn. The lattice constant, $a[\alpha(M/P)]$, of the matrix, i.e. the phase $\alpha(M)$ in contact with various sorts of precipitates, P , depends on the initial Zn content, x , only in case of fully coherent P , i.e. GP zones. In other cases, where P 's are semicoherent or incoherent α'_R , α' or $\beta(\text{Zn})$ phases, $a[\alpha(M/P)]$ is independent of x , but increases with diminishing degree of coherency. The difference in the Zn content between P and $\alpha(M)$ determines the observed changes of the lattice constant.

1. Introduction

Solid solubility of Zn in Al amounts ≈ 1 at% at room temperature, (RT), and ≈ 67 at% at 380 °C. The alloys rapidly quenched from the solid-solution

temperature, T_{ss} ($T_{ss} = 351.5$ °C for the alloy with the zinc content $x = 39.5$ at%), to RT are two-phase systems (at least up to $x \approx 44$ at%), consisting of the FCC α (M/GPZ) phase (M=matrix) in a metastable equilibrium with a dilute system of Guinier–Preston zones (GPZ), having ≈ 70 at%Zn. The (longest) precipitation sequence in supersaturated quenched alloys on ageing is: spherical GPZ (FCC)-ellipsoidal GPZ (FCC)- α'_R (rhombohedrally distorted FCC)- α' (FCC)- β (Zn)(hexagonal). After completion of the precipitation process, FCC α (M/ β) phase, depleted in Zn, is in equilibrium with β (Zn) precipitates, containing ≈ 99 at%Zn [1].

Recent investigations [2-5] proved that precise determination of the position of the diffraction lines of decomposing Al-Zn alloys by X-ray diffraction (XRD) methods is very useful to obtain information, e.g. about the zinc content, x , in the matrix, M, for different types of precipitates, P, in contact with it, and the effect of strains occurring at the precipitate/matrix interface, on the lattice constant of the matrix, $a[\alpha(M/P)]$. The respective results will be briefly summarized together with the most important results reported in the literature.

2. Experimental

A series of Al-Zn alloys with Zn contents up to 48 at%, produced from components of purity 4N, were prepared as (i) fine powders by filing thin foils of about 0.15 mm in thickness, having particle sizes between 10 and 50 μm (powder for short) and (ii) thin needles, cut-off from the foils, with approximate size of 5 mm \times 0.20 mm \times 0.15 mm (needles for short).

The diffraction patterns of the powders were taken at RT, and at elevated temperatures, T , using a counter diffractometer, having a high-temperature attachment, a proportional counter and using graphite-monochromatized $\text{CuK}\alpha_1\alpha_2$ radiation. The needles were investigated in a Debye-Scherrer camera, having a diameter of 114.8 mm, utilizing the spectral $\text{CuK}\alpha_1\alpha_2$ doublets of the 511+333 and 422 matrix diffraction lines at the Bragg angles $> 81^\circ$ and 68° , respectively. All precautions were taken into account in order to minimize the systematic aberrations influencing the diffraction line positions [6], as well as in manipulation with the needles, preventing any transfer of heat to them. The samples were exposed either to air (10^5 Pa) or to a high vacuum (10^{-3} Pa), but no effect of oxidation on diffraction was observed. Several experiments were run with each alloy and quite reproducible results were obtained.

Various heat treatments, HT, were applied:

HT1: The samples were annealed in the range of solid solution at T ranging from 300 to 500 °C for 1h, and quenched inside the furnace in water of RT (free fall distance of about 10 mm; the water was inserted into the furnace just before the quench started). The diffraction patterns in the Debye-Scherrer camera were taken within 3 h after quenching or the Bragg angles of prominent diffraction lines were determined within 0.5 h by means of the counter diffractometer. This treatment will be abbreviated by "as-quenched, T ".

HT2: The samples were slowly cooled within the switched-off furnace from T to RT (“slowly cooled from T ”).

HT3: The as-quenched samples were stored at 250 °C for 5d and subsequently cooled to RT within 15 d; (“slowly cooled from 250 °C”).

HT4: The samples were heated from RT to T with a rate of 2 or 3 K/min; (“heated to T ”).

3. Results and discussion

3.1. RT-values

The RT-values of the lattice constant of the α -matrix in contact with precipitates of the α'_R - and α'_m - (or α' -) phase, $a[\alpha(\text{M/P})]$, $\text{P} = \alpha'_R$ or α' , grown at elevated temperatures between $T = 150$ and 290 °C in Al-Zn alloys ranging in Zn content between $x = 7$ and 30 at%, are given in Ref. 1 (Tables 3.2,3 and 3.2,4, Figs. 3.2,12 and 3.2,17). As was expected from the phase diagram and thermodynamic laws, the plot of $a[\alpha(\text{M/P})]$ versus T fits a smooth interpolating line, in spite of the fairly large differences in the Zn content of the alloys. This result proves that for these sorts of precipitates, $a[\alpha(\text{M/P})]$ is independent of the alloy composition. Of course, the same is true for the lattice constant of both of the considered sorts of precipitates, $a[\text{P}]$.

The lattice constant of the matrix in contact with precipitates of hexagonal β -phase was recently determined [2-5]. The nine Al-Zn alloys had the Zn content between $x = 8$ and 44 at%. The samples were “slowly cooled from $T = 400$ °C; HT2”. Independently of the alloy composition, $a[\alpha(\text{M}/\beta)] = 0.40445(10)$ nm was obtained. When the powders were quenched from 400 °C in water at RT (HT1) and subsequently aged for a long time at RT or at 80 °C, $a[\alpha(\text{M}/\beta)] = 0.40469(6)$ nm was obtained (p.275, Figs. 7-9,11, Table 1 in Ref. 3). From the phase diagram given in the review of Murray [7], the Zn content of the matrix in contact with the $\beta(\text{Zn})$ equilibrium phase, $\alpha(\text{M}/\beta)$ is $x[\alpha(\text{M}/\beta)] = (1.0 \pm 0.3)$ at%. From the plot of the lattice constant of the α -phase versus the Zn content of the alloy, presented in Fig. 4 in Ref. 3, for this Zn content of the matrix one has to expect $a[\alpha(\text{M}/\beta)] = 0.40485(3)$ nm. This value is about 0.04% higher than the measured one. The difference is larger than the experimental error. According to the fitting curve, at RT, $a[\alpha(x)]$ can be extrapolated by

$$a[\alpha(x)] = (0.40494 - 0.854 \times 10^{-4} x/\text{at}\%) \text{ nm.} \quad (1)$$

The explanation for this deviation is the following. As they begin to appear, the $\alpha(\text{M}/\beta)$ diffraction lines are very broad (see, e.g. Figs. 8,9 in Ref. 3), i.e. the matrix is in a strained condition. The supposed reason is that approximately at $T < 85$ °C (see Chapt. 3.3.1 in Ref. 1) the precipitates of the $\beta(\text{Zn})$ -phase should be predominantly nucleated at GP zones. As demonstrated in Chapt. 3.2.5. and 3.2.6 in Ref. 1, this transformation may start with the formation of stacking faults

or microlamellae of hexagonal structure on (111) planes of the GP zones, resulting in $(001)_{\beta} \parallel (111)_{\text{GPZ}}$, in accordance with the orientation relationship between the $\beta(\text{Zn})$ - and $\alpha(\text{M}/\beta)$ -phase. Using $a[\alpha(\text{M}/\beta)] = 0.4047 \text{ nm}$ and $c(\beta) = 0.4947 \text{ nm}$, it follows that $3c(\beta) \approx 2\sqrt{3}a[\alpha(\text{M}/\beta)]$ with a misfit of only about 5.5%. As a consequence, the initial $\beta(\text{Zn})$ particles are fairly small and not totally incoherent to $\alpha(\text{M}/\beta)$, since part of their (001) planes should continue in the matrix as $\{111\}$ planes. The maintenance of a certain degree of coherency is associated with a distortion of the lattice surrounding the precipitates. The observed difference in $a[\alpha(\text{M}/\beta)]$ between the measured value, i.e. $0.40469(6) \text{ nm}$, and the expected one, namely $0.40485(3) \text{ nm}$, is caused by the partial coherence of part of the $(001)_{\beta}$ planes, since this effect is associated with a certain increase of the amount of solute atoms dissolved in the matrix.

In the alloy with $x = 4.5 \text{ at\%}$, slowly cooled from $250 \text{ }^{\circ}\text{C}$ to RT (HT3), diffraction lines of the α -matrix and of the $\beta(\text{Zn})$ -phase were observed. The determined lattice constant of the matrix is $a[\alpha(\text{M}/\beta)] = 0.40448(3) \text{ nm}$. Independent of the Zn content of the alloys, this value is smaller than the lattice constant of the α -matrix in thermodynamic equilibrium with the $\beta(\text{Zn})$ -phase, i.e. $a[\alpha(\text{M}/\beta)]_{eq} = 0.40469(6) \text{ nm}$. During cooling, only part of the zinc atoms dissolved in excess at RT in the matrix form precipitates of the $\beta(\text{Zn})$ -phase. The assumed reason is that (according to the phase diagram, p. 101 in Ref. 1) for the Al-4.5 at% Zn alloy, the two-phase ($\alpha - \beta$) region is passed at about $180 \text{ }^{\circ}\text{C}$ during cooling. As a result, the amount of excess vacancies is small and the mobility of zinc atoms is also small.

Now the lattice constant of the α -phase in contact with GP zones $a[\alpha(\text{M}/\text{GPZ})]$, is considered. The recent results [3-5] are summarized in Table 1. 11 Al-Zn alloys were investigated, with the Zn content between 4.5 and 48 at% and pure Al in the as-quenched state (HT1).

Before discussing these results, some additional information is necessary. For alloys with the Zn content between 4.5 and 40 at%, the diffraction lines of $\alpha(\text{M}/\text{GPZ})$ are fairly sharp with well separated $K\alpha_1\alpha_2$ spectral doublet components, at higher Bragg angles, but still a little broader than those of pure Al. Furthermore, on the high-angle side of diffraction lines of $\alpha(\text{M}/\text{GPZ})$, there is a faint broad hump due to diffraction effects of GP zones (Fig.3 in Ref. 3). The positions of the diffraction lines of $\alpha(\text{M}/\text{GPZ})$ do not change during the coarsening of GP zones. Of course, after storing at RT, diffraction lines of $\alpha(\text{M}/\beta)$ (and $\beta(\text{Zn})$) appear and increase in intensity, and simultaneously those of $\alpha(\text{M}/\text{GPZ})$ start to diminish. As it is shown in Ref. 1 (Chapt. 3.3.1), below $T \approx 85 \text{ }^{\circ}\text{C}$ the (direct) transition of GP-zones into $\beta(\text{Zn})$ is dominant. For the Al-24 at%Zn alloy at RT, the complete transition lasts about 100 d, whereas for the alloy with 48 at% Zn, it takes only about 2 d.

The most striking feature of the measured values of $a[\alpha(\text{M}/\text{GPZ})]$ is that, in contrast to the other kinds of phases, namely α'_R , α'_m and $\beta(\text{Zn})$, they distinctly depend on alloy composition. The values linearly decrease with increasing the initial Zn content of the alloys up to $x = 44 \text{ at\%}$ and they can be fitted by Eq.(1). The measured $a[\alpha(\text{M}/\text{GPZ})]$ is considerably smaller than the one which would be expected from the experimentally determined dissolution line of the GP zones

(see Chapt. 3.8.2 in Ref. 1). Accordingly, at RT, independent of alloy composition, $a[\alpha(\text{M/GPZ})] = (1.7 \pm 0.2)$ at%; according to Eq.(1) resulting in $a(x = 1.7 \text{ at}\%) = 0.40480(5)$ nm.

TABLE 1.

$a[\alpha(\text{M/GPZ})]$ as a function of the zinc content, x , of several Al-Zn alloys for the as-quenched state (HT1), i.e. $T/\text{H}_2\text{O}(\text{RT})/t_{\text{RT}} = 3$ h (for needles) or 0.5 h (for powder). The results were practically the same for both kinds of samples (see Fig. 4 in Ref. 3). $T = 500$ °C for $x = 4.5$ at% and 400 °C for the other alloys [5], [3]. The Guinier radius, r_G , of the GP zones for the alloy with $x = 8$ at% was 2.2 nm and for $x = 24$ at% $r_G = 1.2$ nm [2].

| $x/\text{at}\%$ | $a[\alpha(\text{M/GPZ})]/\text{nm}$ |
|-----------------|-------------------------------------|
| 0 (pure Al) | 0.40494(3) |
| 4.5 | 0.40465(3) |
| 8 | 0.40426(5) |
| 15 | 0.40346(5) |
| 20 | 0.40330(5) |
| 24 | 0.40287(5) |
| 26 | 0.40272(5) |
| 35 | 0.40190(7) |
| 38 | 0.40171(7) |
| 40 | 0.40123(8) |
| 44 | 0.40094(8) |
| 48 | no GP zones |

It is important to note that the $a[\alpha(\text{M/GPZ})]$ values presented in Table 1, and those given in the review of Murray (Table 13 and Fig. 4 in Ref. 7) and indicated as belonging to the “FCC solid solution”, $\alpha(SS)$, fit well a common straight line (see Fig. 4 in Ref. 3). According to SAXS investigations (see, e.g. Fig. 16 in Ref. 3), the formation of GP zones cannot be avoided either in slowly cooled or in quenched samples, if $x > 10$ at%. That means, one can be sure that only up to $x = 10$ at%, $a[\alpha(SS)] = a[\alpha(\text{M/GPZ})]$. For higher contents of Zn, one determines $a[\alpha(\text{M/GPZ})]$, even in the quenched samples, from the beginning of the ageing at RT. The fact that the straight line defined by Eq. (1) fits well the experimentally determined values of $a[\alpha(SS)]$ for $x < 10$ at% and of $a[\alpha(\text{M/GPZ})]$ for alloys with the Zn content between 4.5 and 44 at%, can be taken as an indication that also for the alloys with $x > 10$ at% $a[\alpha(SS)] \approx a[\alpha(\text{M/GPZ})]$. The explanation of the difference between the expected values, namely $a(x = 1.7 \text{ at}\%) = 0.40480$ nm, and the measured ones presented in Table 1, is that in the Al-Zn alloys containing a sufficiently dense system of GP zones, the lattice spacing in the matrix, $a[\alpha(\text{M/GPZ})]$, is lowered with respect to $a(x = 1.7 \text{ at}\%)$ in order to reduce the (positive) contributions of the coherency strains to the total free energy [2,3]. This effect increases with increasing the volume fraction of the GP zones.

3.2. Lattice constants at elevated temperatures

Quite recently, the lattice constant of the Al-rich matrix, $a[\alpha(M/P)]$, in contact with precipitates of the metastable FCC α'_m -phase and the $\beta(\text{Zn})$ equilibrium phase was studied in four Al-Zn alloys, with $x = 8, 24, 40$ and $48\text{at}\%$, between RT and 400°C by X-ray powder diffraction [4] (Fig. 1). The results will be discussed together with the literature data [8-10].

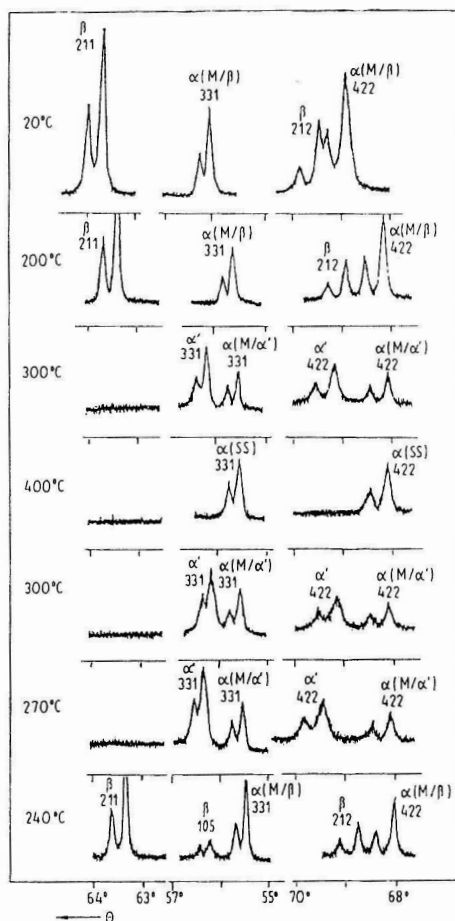


Fig. 1. Prominent diffraction lines of the (annealed) alloy Al-40 at%Zn at different temperatures, including both heating and cooling cycles. One can notice thermal expansion of the phases present, a change in the Zn content in the phases, a decrease of diffraction line intensities due to increased thermal vibration amplitudes with temperature, phase transitions $\beta(\text{Zn})-\alpha'$ (at 277°C) and $\alpha'-\beta(\text{Zn})$ (at 260°C), and formation of solid solution, $\alpha(SS)$ (400°C).

As outlined in Ref. 1 (Chapt.3.2.4), the precipitates of the α'_m -phase have a

fairly high degree of coherency; they are semicoherent. The degree of coherency of the α'_m - or α' -phase is placed between those of the GP zones and of the hexagonal β (Zn) equilibrium phase.

TABLE 2.

Values used to calculate the average expansion coefficient $\alpha = [\Delta a/\bar{a}]/\Delta T$, δa being the difference and \bar{a} the average of the values in the 3rd and 2nd columns. The value denoted with the asterisk was found by extrapolation (Fig. 4 in Ref. 3).

| $x/\text{at}\%$ | $a[\alpha(\text{M/GPZ})]$ at 20 °C (nm) | Ref. | $a[\alpha(SS)]$ at 400 °C (nm) | Ref. | $10^5\alpha/\text{K}^{-1}$ | a (nm) |
|-----------------|--|------|-----------------------------------|------|----------------------------|----------|
| 0 | 0.40494(2) | [4] | 0.40952(6) | [4] | 3.0(1) | 0.40723 |
| 8 | 0.40426(5) | [3] | 0.40925(8) | [4] | 3.2(2) | 0.40676 |
| 24 | 0.40287(5) | [3] | 0.40824(7) | [4] | 3.5(1) | 0.40556 |
| 40 | 0.40123(8) | [3] | 0.40692(9) | [4] | 3.7(2) | 0.40408 |
| 48 | 0.40065(10)* | [3] | 0.40584(6) | [4] | 3.4(2) | 0.40325 |

For the following consideration, information about the average thermal expansion coefficients, $\alpha[\Delta a/a]/\Delta T$, as a function of the Zn content of the alloys are needed. The data applied to evaluate *alpha* are presented in Table 2.

TABLE 3.

Information on: (i) the zinc content of the α'_m - (i.e. α' -) phase, $x[\alpha']$, in (metastable) equilibrium with the matrix having the zinc content $x[\alpha(\text{M}/\alpha')]$ [10]; (ii) the lattice constants $a[\alpha(\text{M}/\alpha')]$ and $a[\alpha']$ measured at RT (see Table 1 in Ref. 8; (iii) the lattice constants given in (ii), but extrapolated to the respective T using the thermal expansion coefficients presented in Table 2, and values taken "in situ" at T (denoted with asterisks), in dependence upon T . For zinc contents higher than 48 at%, $a = 0.402$ nm and $\alpha = 3.3 \times 10^{-5}/\text{K}$ were applied.

| $T/\text{°C}$ | (i) | | (ii) | | (iii) | |
|---------------|-------------------------------|--------------|-------------------------------|--------------|-------------------------------|--------------|
| | $x[\alpha(\text{M}/\alpha')]$ | $x[\alpha']$ | $a[\alpha(\text{M}/\alpha')]$ | $a[\alpha']$ | $a[\alpha(\text{M}/\alpha')]$ | $a[\alpha']$ |
| | (at%) | | (taken at RT) | | (at T) | |
| 170 | 6.2 | 68.5 | 0.40450 | 0.39960 | 0.40645 | 0.40160 |
| 180 | 6.6 | 67.9 | 0.40450 | 0.39960 | 0.40660 | 0.40170 |
| 190 | 7.8 | 67.2 | 0.40440 | 0.39960 | 0.40660 | 0.40185 |
| 200 | 8.0 | 66.5 | 0.40435 | 0.39960 | 0.40670 | 0.40200 |
| 230 | 10.7 | 64.0 | 0.40415 | 0.39950 | 0.40690 | 0.40230 |
| 250 | 12.9 | 62.0 | 0.40375 | 0.39950 | 0.40674 | 0.40255 |
| 260 | 14.1 | 61.0 | 0.40340 | 0.39950 | 0.40655 | 0.40270 |
| 270 | 15.5 | 59.7 | | | 0.40700(7)* | 0.40315(8)* |
| 290 | 18.6 | 57.3 | 0.40280 | 0.39940 | 0.40655 | 0.40300 |
| | | | | | 0.40696(7)* | 0.40365(7)* |
| 300 | 20.5 | 55.9 | | | 0.40695(8)* | 0.40388(7)* |
| 340 | 30.9 | 47.4 | | | 0.40685(8)* | 0.40482(9)* |

In Table 3.2,4 and Fig. 3.2,17 of Ref.1, the information about $a[\alpha'_m]$ (or $a[\alpha']$) as well as $a[\alpha(M/\alpha')]$ as a function of the temperature, T , at which the precipitates were grown, is given for Al-Zn alloys with Zn contents between 11 and 30 at%. The lattice constants were determined at RT by XRD methods mostly. In Ref. 4, however, they were measured "in situ" at 270, 290, 300 and 340 °C (Fig.1). Using the values of α presented in Table 2, one can extrapolate the data taken at RT to the respective T at which the alloys actually decomposed, and compare them with the "in situ" values (Table 3).

Inspecting the data of $a[\alpha']$ in dependence on T presented in the last column of Table 3, a "jump" between the last extrapolated value (i.e. at 290 °C) and the ones determined "in situ", is noticed. It is supposedly due to the increase of the Zn content of the α' -precipitates during the quench from T to RT and during the storing at RT in particular, which causes a decrease of $a[\alpha']$. In addition, the uncertainties of the average thermal expansion coefficients might also contribute to this "jump".

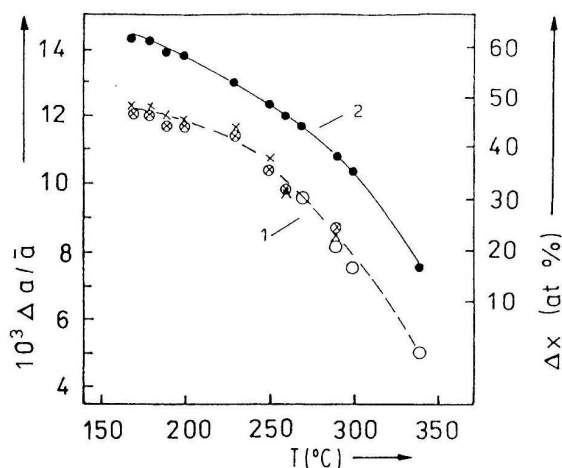


Fig. 2. Curve 1: Relative difference between $a[\alpha(M/\alpha')]$ and $a[\alpha']$ as a function of T ; the crosses belong to the values determined at RT (4th and 5th column in Table 3), the circles with a cross to the ones extrapolated from RT to T (6th and 7th column in Table 3) and the bare circles to the ones measured "in situ" at T [4]. Curve 2: The difference in the Zn content, Δx , of the phases α' and $\alpha(M/\alpha')$ as a function of T , solid circles.

In Fig. 2 the relative differences of $a[\alpha']$ and $a[\alpha(M/\alpha')]$ are drawn versus T for both, the values measured at RT and those extrapolated to T or measured "in situ" at T . In addition, the difference Δx of the Zn content of the two considered α -phases is presented. Since the differences between $\Delta a/\bar{a}$, determined from the values measured at RT and those extrapolated to or measured at T are within the range of experimental error, they are fitted by a common (dashed) curve (Curve

1). Curve 1 is approximately running in parallel to Curve 2, representing Δx as a function of T . Thus, one can conclude that the difference in lattice spacing between the α' - and $\alpha(\text{M}/\alpha')$ -phases and its dependence on T , is mainly determined by their Zn contents.

The thermal expansion of $\beta(\text{Zn})$ is anisotropic: $\alpha(a) = 1.1(1) \times 10^{-5}/\text{K}$ and $\alpha(c) = 8.5(9) \times 10^{-5}/\text{K}$. That means the c/a -value slightly increases from 1.86 at RT to 1.89 at $T = 270$ °C [4].

4. Conclusion

Comparing the lattice constant, $a[\alpha(\text{M}/\text{P})]$, of the matrix in contact with various sorts of precipitates, P, the following conclusion can be drawn. Only in the case of fully coherent P's that are GP zones, $a[\alpha(\text{M}/\text{GPZ})]$ strongly depends on the Zn content, x . In other cases, namely, the matrix in contact with rhombohedrally distorted FCC α'_R phase (having one extra $\{111\}$ plane with respect to the matrix), the FCC α' phase, being semicoherent, and finally the incoherent hexagonal $\beta(\text{Zn})$ phase, $a[\alpha(\text{M}/\text{P})]$ is independent of x . It holds that $a[\alpha(\text{M}/\text{P})]$ increases with diminishing degree of coherency [2-4,9].

Acknowledgement

The authors gratefully acknowledge the support of the U.S.A. (National Institute of Standards and Technology)–Croatia (Ministry of Science and Technology) Joint Fund (grant No. JF 106) in this study.

References

- 1) *Structure and Structure Development of Al-Zn Alloys*, Editor H.Löffler (Akademie Verlag, Berlin, 1995);
- 2) S. Popović, H.Löffler, B.Gržeta, G.Wendrock and P.Czurratis, *Phys. Stat. Sol. (a)* **111** (1989) 417;
- 3) S. Popović, B. Gržeta, V. Ilakovac, R. Kroggel, G. Wendrock and H. Löffler, *Phys. Stat. Sol. (a)* **130** (1992) 273;
- 4) S. Popović, B. Gržeta, H. Löffler and G. Wendrock, *Phys. Stat. Sol. (a)* **140** (1993) 341;
- 5) S. Popović, B.Gržeta, V.Ilakovac, H. Löffler and G.Wendrock, *Phys. Stat. Sol. (a)* **141** (1994) 43;
- 6) S. Popović, *Cryst. Res. Technol.* **20** (1985) 552;
- 7) J. L. Murray, *Bull. Alloy Phase Diagrams* **4** (1983) 55;
- 8) M.Werner and H. Löffler, *Cryst. Res. Technol.* **18** (1983) 459;
- 9) M. Werner, R. Ramlau and H. Löffler, *Cryst. Res. Technol.* **18** (1983) 599;
- 10) H. Löffler, C. Eschrich and O. Simmich, *Phys. Stat. Sol. (a)* **113** (1989) 269.

KONSTANTA KRISTALNE REŠETKE FAZE α U RAVNOTEŽI S RAZNIM
PRECIPITATIMA U SLITINAMA Al-Zn

Niz slitina Al-Zn u području bogatom Al istraživano je rentgenskom difrakcijom pri sobnoj i povišenoj temperaturi. Prema rezultatima sadašnjeg rada i literaturnih podataka može se izvesti sljedeći zaključak. Konstanta rešetke, $a[\alpha(M/P)]$, matrice, tj. faze $\alpha(M)$ u ravnoteži s raznim vrstama precipitata, P, ovisi o početnom udjelu Zn, x , samo u slučaju potpuno koherentnih P, tj. GP zona. U ostalim slučajevima, gdje su P polukoherentne ili nekoherentne faze α'_R , α' ili $\beta(Zn)$, $a[\alpha(M/P)]$ ne ovisi o x , ali raste sa smanjivanjem stupnja koherencije. Razlika u x između P i $\alpha(M)$ određuje opažene promjene konstante rešetke.